

视觉有向目标的高精度检测

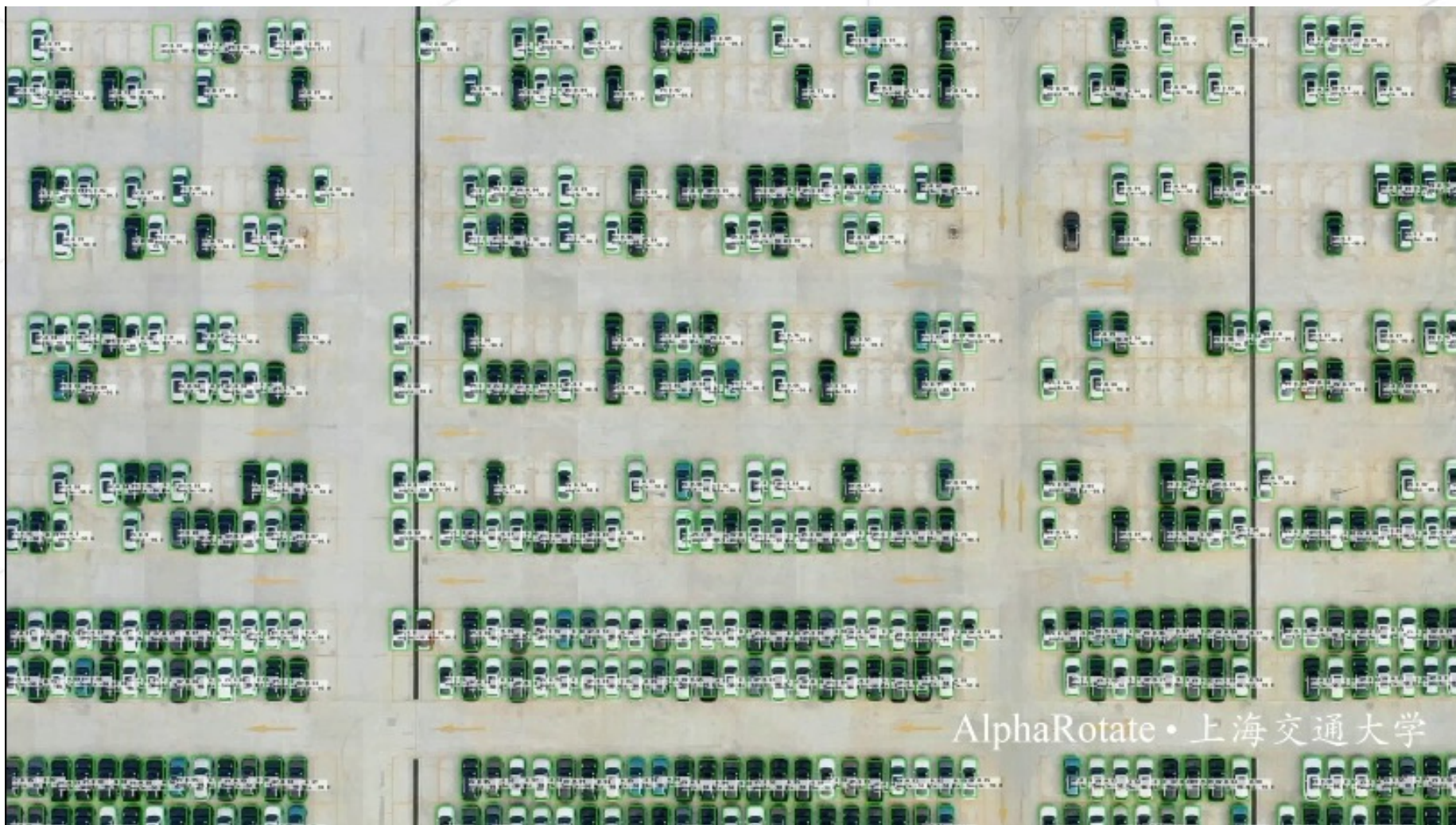
杨学 上海交通大学

2022/07/07

【OpenMMLab 社区开放麦】是由 OpenMMLab 发起，面向所有社区成员的社区分享直播活动，每周四晚八点准点播出。旨在搭建一个知识分享的舞台，在这里，社区里的每个人都能拿起话筒分享你的知识和见解。我们一直认为，分享与交流能更好地促进知识的传播；平等与共建能更好地维持社区的氛围。

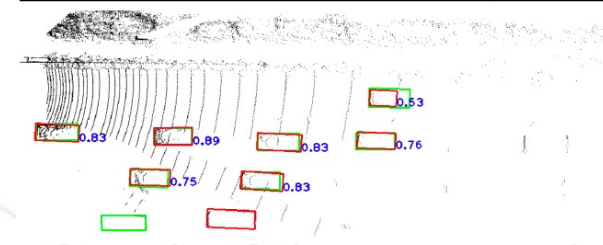
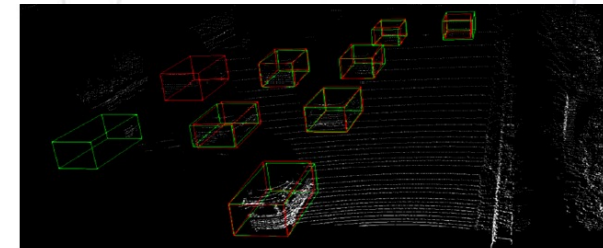
1. 有向目标检测
2. 问题和挑战
3. 解决方法
4. 实验分析

- 预测具有方向的边界框并对目标进行识别



应用场景

- 遥感检测
- 人脸检测
- 零售场景检测
- 场景文字检测
- 3D目标检测



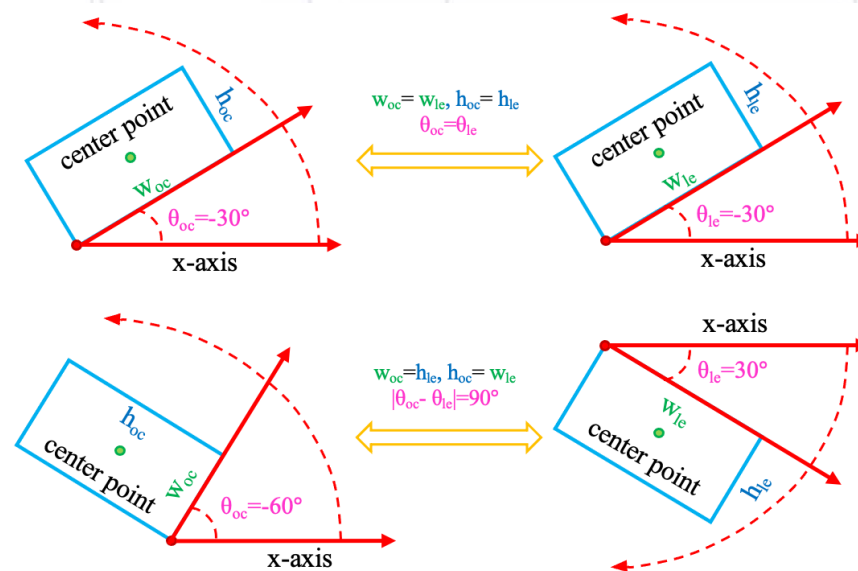
旋转框的定义方式：

- OpenCV定义法： $(x, y, w_{oc}, h_{oc}, \theta_{oc}), \theta_{oc} \in [-90, 0)$
- 长边定义法： $(x, y, w_{le}, h_{le}, \theta_{le}), \theta_{le} \in [-90, 90)$

转换关系：

$$D_{le}(w_{le}, h_{le}, \theta_{le}) = \begin{cases} D_{oc}(w_{oc}, h_{oc}, \theta_{oc}), & w_{oc} \geq h_{oc} \\ D_{oc}(h_{oc}, w_{oc}, \theta_{oc} + 90^\circ), & otherwise \end{cases}$$

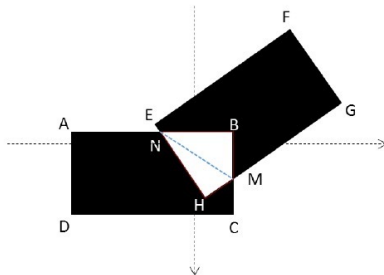
$$D_{oc}(w_{oc}, h_{oc}, \theta_{oc}) = \begin{cases} D_{le}(w_{le}, h_{le}, \theta_{le}), & \theta_{le} \in [-90^\circ, 0^\circ) \\ D_{le}(h_{le}, w_{le}, \theta_{le} - 90^\circ), & otherwise \end{cases}$$



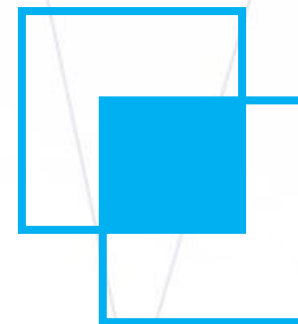
旋转框IoU的计算：

Algorithm 1 IoU computation

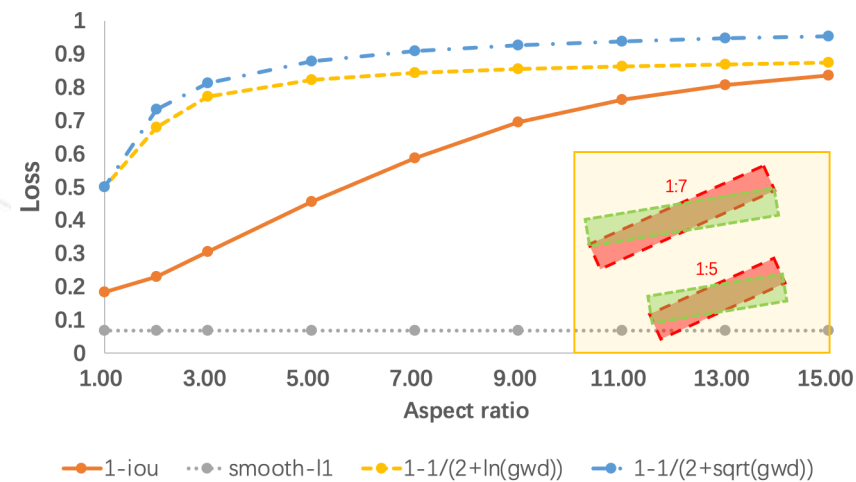
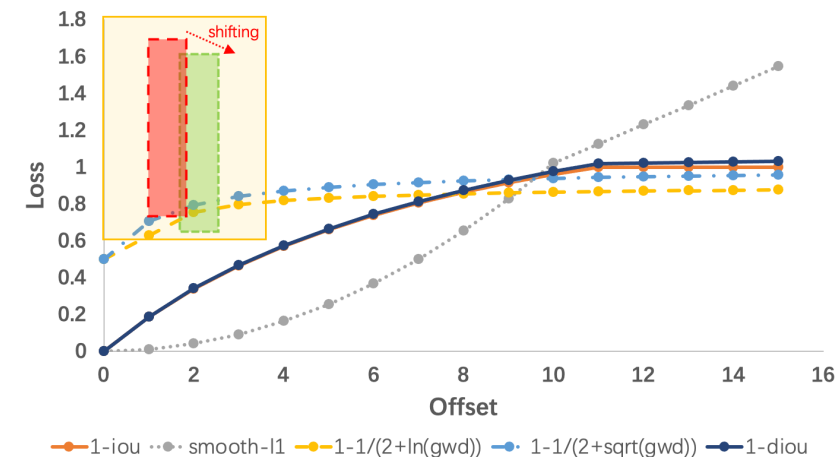
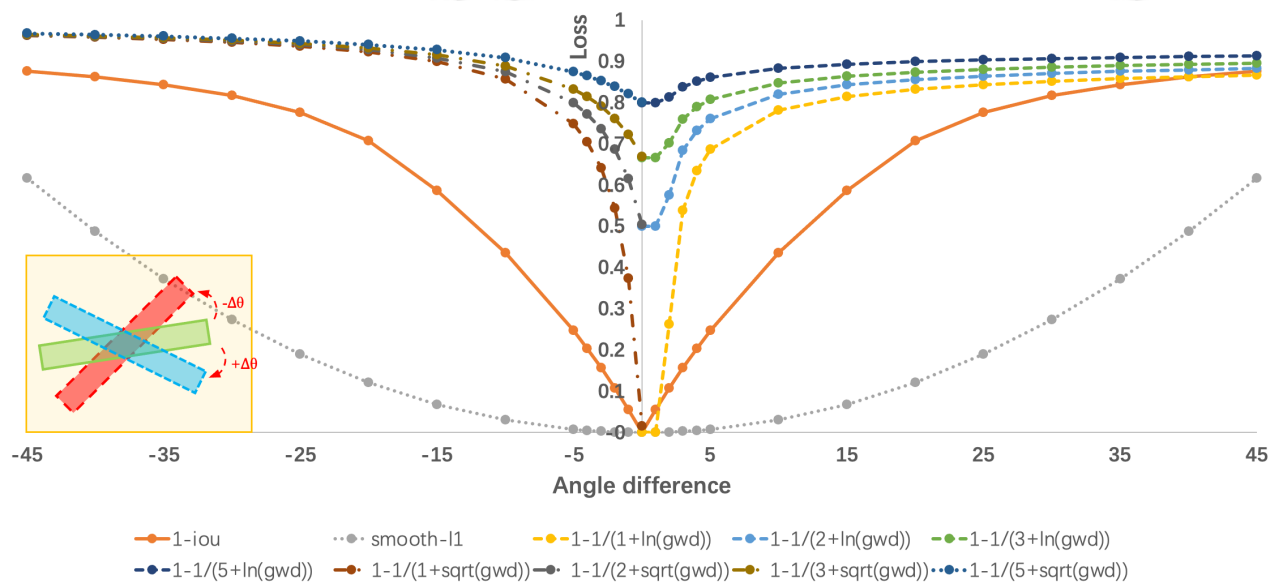
- 1: Input: Rectangles R_1, R_2, \dots, R_N
 - 2: $\text{IoU}[1, N][1, N] \leftarrow 0$
 - 3: **for** each pair of R_i, R_j ($i < j$) **do**
 - 4: Point set $PSet \leftarrow \emptyset$
 - 5: Add intersection points of R_i and R_j to $PSet$
 - 6: Add the vertices of R_i inside R_j into $PSet$
 - 7: Add the vertices of R_j inside R_i into $PSet$
 - 8: Sort $PSet$ to anti-clockwise order
 - 9: Compute intersection I of $PSet$ by triangulation
 - 10: $\text{IoU}(i, j) \leftarrow (\text{Area}(R_i) + \text{Area}(R_j) - I)/I$
 - 11: **end for**
 - 12: return IoU
-



$$\text{IoU} = \frac{\text{Area of Overlap}}{\text{Area of Union}}$$

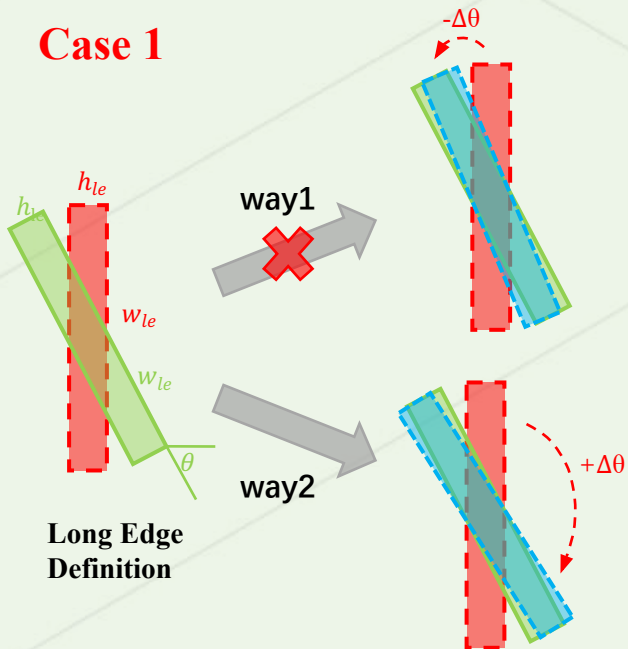


评估与损失不一致问题



边界不连续问题

Case 1



长边定义法

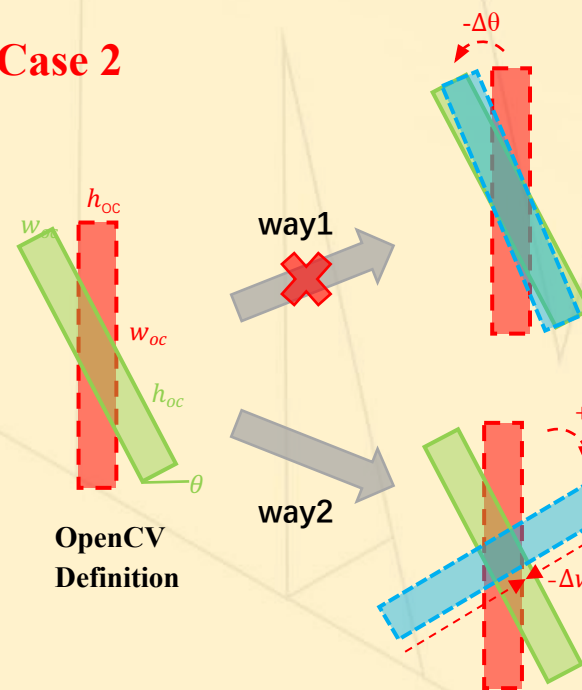
Anchor/Proposal: $(0,0,70,10,-90^\circ)$
Ground-Truth: $(0,0,70,10,65^\circ)$
Predict box: $(0,0,70,10,-115^\circ)$

$w = w, h = h, |\theta - \theta| = 180^\circ$
 $\text{IoU} < \mathbf{G}, \mathbf{P} \approx 1$
Smooth-L1 Loss $< \mathbf{G}, \mathbf{P} > \text{PoA} \gg 0$

Anchor/Proposal: $(0,0,70,10,-90^\circ)$
Ground-Truth: $(0,0,70,10,65^\circ)$
Predict box: $(0,0,70,10,65^\circ)$

$w = w, h = h, |\theta - \theta| = 0^\circ$
 $\text{IoU} < \mathbf{G}, \mathbf{P} \approx 1$
Smooth-L1 Loss $< \mathbf{G}, \mathbf{P} \approx 0$

Case 2



OpenCV定义法

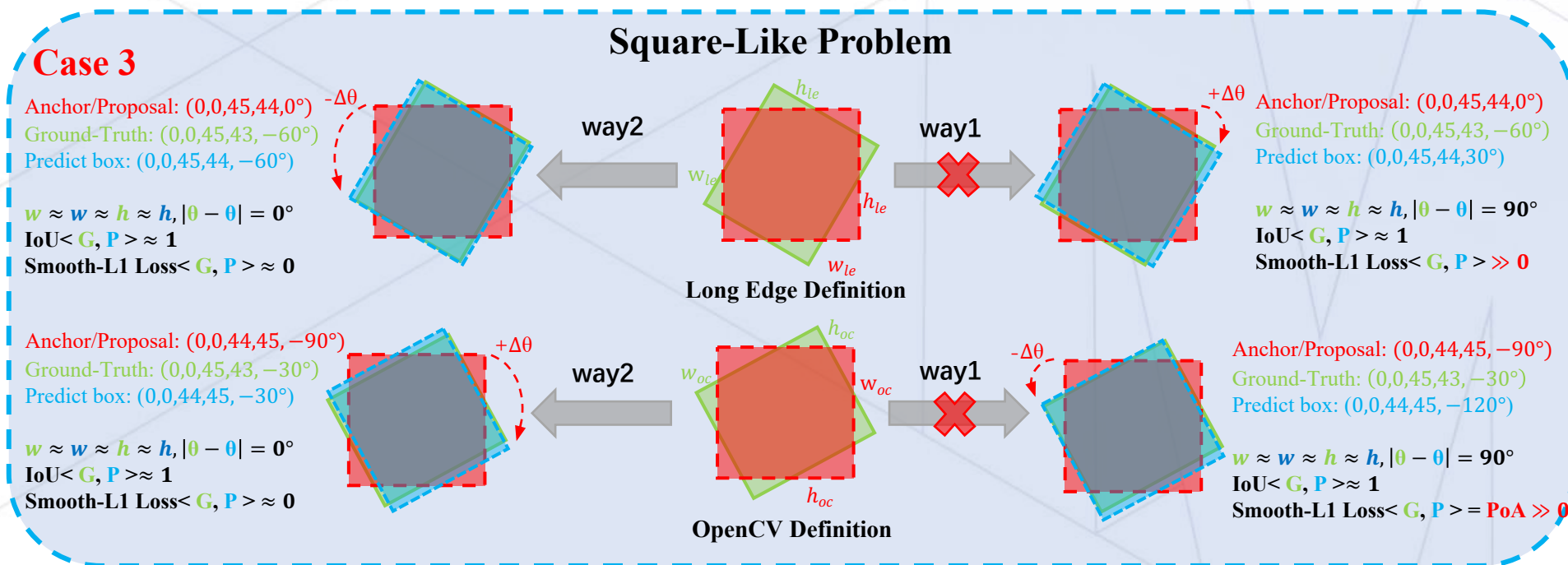
Anchor/Proposal: $(0,0,70,10,-90^\circ)$
Ground-Truth: $(0,0,10,70,-25^\circ)$
Predict box: $(0,0,70,10,-115^\circ)$

$w = h, h = w, |\theta - \theta| = 90^\circ$
 $\text{IoU} < \mathbf{G}, \mathbf{P} \approx 1$
Smooth-L1 Loss $< \mathbf{G}, \mathbf{P} > \text{PoA} + \text{EoE} \gg 0$

Anchor/Proposal: $(0,0,70,10,-90^\circ)$
Ground-Truth: $(0,0,10,70,-25^\circ)$
Predict box: $(0,0,10,70,-25^\circ)$

$w = w, h = h, |\theta - \theta| = 0^\circ$
 $\text{IoU} < \mathbf{G}, \mathbf{P} \approx 1$
Smooth-L1 Loss $< \mathbf{G}, \mathbf{P} \approx 0$

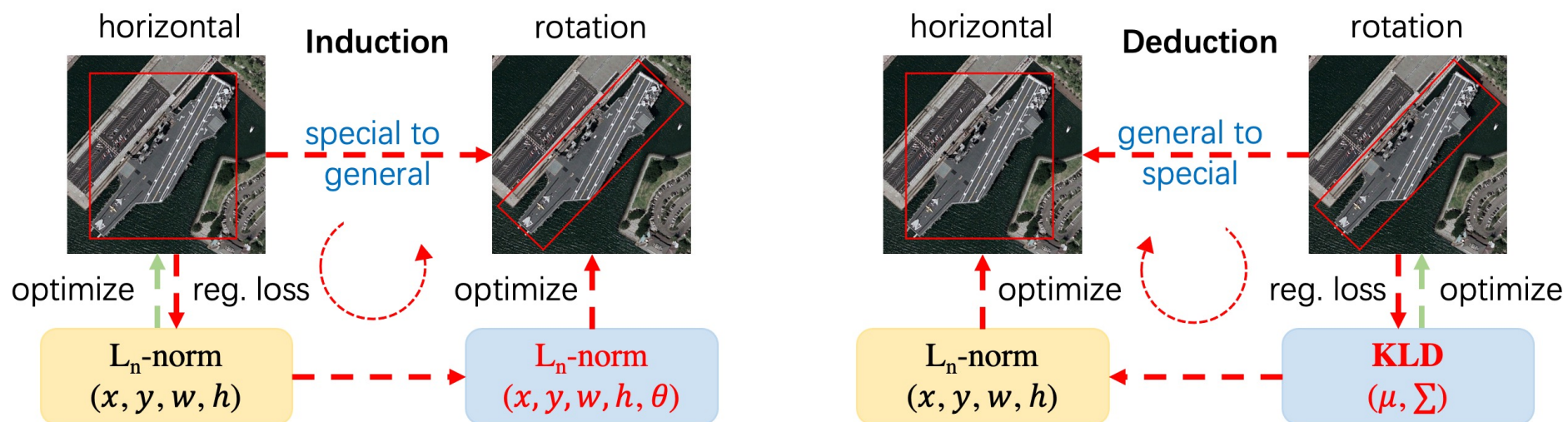
类正方形检测问题



长宽比越小，IoU对角度越不敏感

有向目标检测器的两种设计范式

- 归纳范式
- 演绎范式



X. Yang, et al. "Rethinking Rotated Object Detection with Gaussian Wasserstein Distance Loss." In ICML 2021.

X. Yang, et al. "Learning High-Precision Bounding Box for Rotated Object Detection via Kullback-Leibler Divergence." In NeurIPS 2021.

归纳范式

- 对于常见的通用检测模型（水平框检测），模型通常是通过回归四个偏移量的形式来进行框位置和大小的预测：

$$t_x^p = \frac{x_p - x_a}{w_a}, t_y^p = \frac{y_p - y_a}{h_a}, t_w^p = \ln\left(\frac{w_p}{w_a}\right), t_h^p = \ln\left(\frac{h_p}{h_a}\right)$$

来匹配实际的偏移量：

$$t_x^t = \frac{x_t - x_a}{w_a}, t_y^t = \frac{y_t - y_a}{h_a}, t_w^t = \ln\left(\frac{w_t}{w_a}\right), t_h^t = \ln\left(\frac{h_t}{h_a}\right)$$

- 借鉴于此，目前绝大多数的旋转目标检测在上面的基础上加上了角度参数的回归：

$$t_\theta^p = f(\theta_p - \theta_a), t_\theta^t = f(\theta_t - \theta_a)$$

归纳范式

- 然后回归损失也常采用Ln-norm：

$$L_{reg} = l_n\text{-norm}(\Delta t_x, \Delta t_y, \Delta t_w, \Delta t_h, \Delta t_\theta)$$

where $\Delta t_x = t_x^p - t_x^t = \frac{\Delta x}{w_a}$, $\Delta t_y = t_y^p - t_y^t = \frac{\Delta y}{h_a}$, $\Delta t_w = t_w^p - t_w^t = \ln(w_p/w_t)$, $\Delta t_h = t_h^p - t_h^t = \ln(h_p/h_t)$, and $\Delta t_\theta = t_\theta^p - t_\theta^t = \Delta\theta$.

- 五个参数的优化和目标本身形状等关联不大，使得我们需要根据不同的数据集特点进行权重的调整。比如大长宽比目标可能需要着重关注角度参数，小目标则需要关注中心点参数，因此这些参数的轻微偏移都会造成这些目标预测精准度（IoU）的急剧下降。

演绎范式

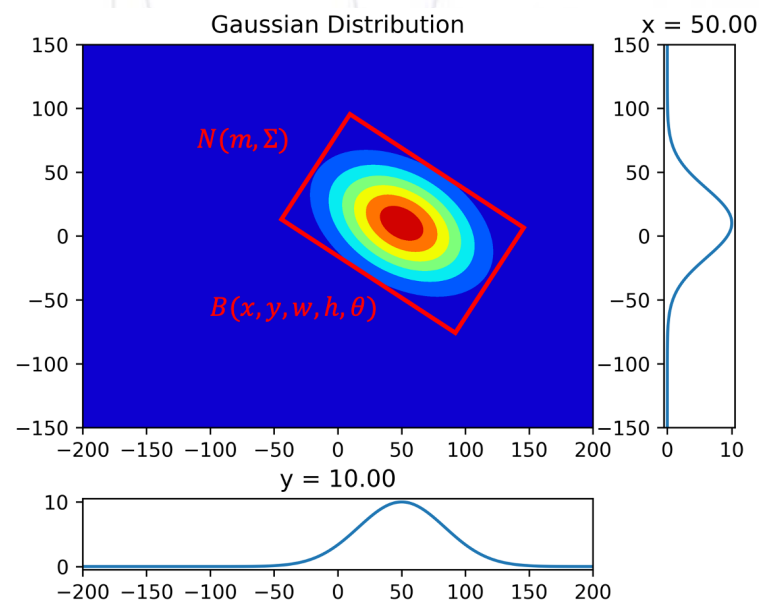
- 要求 1：与 IoU 度量高度一致
- 要求 2：易实现、可微分允许直接学习
- 要求 3：在角度边界情况下平滑

Property 1: $\Sigma^{1/2}(w, h, \theta) = \Sigma^{1/2}(h, w, \theta - \frac{\pi}{2})$;

Property 2: $\Sigma^{1/2}(w, h, \theta) = \Sigma^{1/2}(w, h, \theta - \pi)$;

Property 3: $\Sigma^{1/2}(w, h, \theta) \approx \Sigma^{1/2}(w, h, \theta - \frac{\pi}{2})$, if $w \approx h$.

$$\begin{aligned}\Sigma^{1/2} &= \mathbf{R}\mathbf{S}\mathbf{R}^\top \\ &= \begin{pmatrix} \cos \theta & -\sin \theta \\ \sin \theta & \cos \theta \end{pmatrix} \begin{pmatrix} \frac{w}{2} & 0 \\ 0 & \frac{h}{2} \end{pmatrix} \begin{pmatrix} \cos \theta & \sin \theta \\ -\sin \theta & \cos \theta \end{pmatrix} \\ &= \begin{pmatrix} \frac{w}{2} \cos^2 \theta + \frac{h}{2} \sin^2 \theta & \frac{w-h}{2} \cos \theta \sin \theta \\ \frac{w-h}{2} \cos \theta \sin \theta & \frac{w}{2} \sin^2 \theta + \frac{h}{2} \cos^2 \theta \end{pmatrix} \\ \mathbf{m} &= (x, y)^\top\end{aligned}$$



Wasserstein Distance

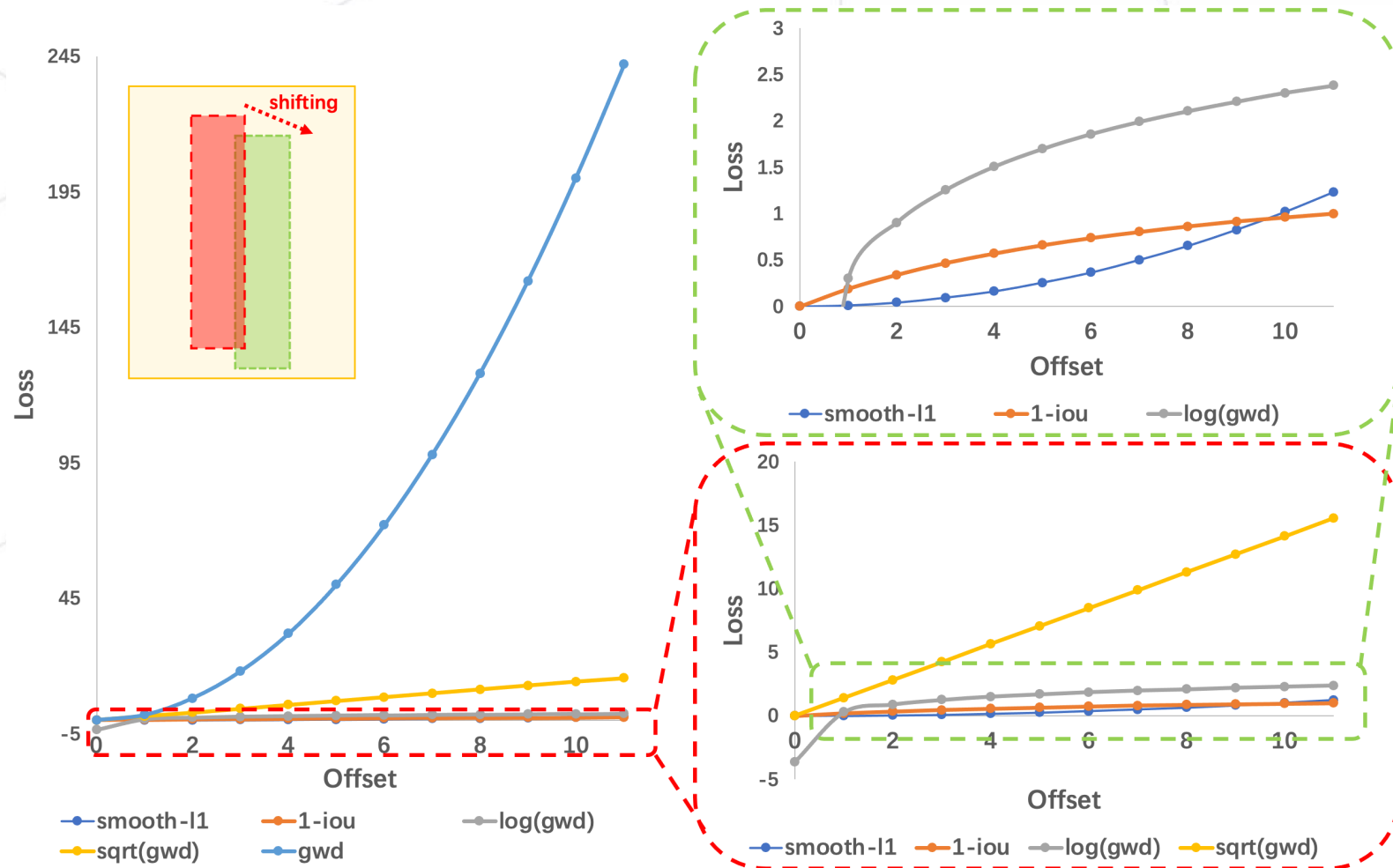
- 通用公式：

$$\mathbf{D}_w(\mathcal{N}_p, \mathcal{N}_t)^2 = \underbrace{\|\boldsymbol{\mu}_p - \boldsymbol{\mu}_t\|_2^2}_{\text{center distance}} + \underbrace{\text{Tr}(\boldsymbol{\Sigma}_p + \boldsymbol{\Sigma}_t - 2(\boldsymbol{\Sigma}_p^{1/2} \boldsymbol{\Sigma}_t \boldsymbol{\Sigma}_p^{1/2})^{1/2})}_{\text{coupling terms about } h_p, w_p \text{ and } \theta_p}$$

- 水平特殊情况：

$$\begin{aligned} \mathbf{D}_w^h(\mathcal{N}_p, \mathcal{N}_t)^2 &= \|\boldsymbol{\mu}_p - \boldsymbol{\mu}_t\|_2^2 + \|\boldsymbol{\Sigma}_p^{1/2} - \boldsymbol{\Sigma}_t^{1/2}\|_F^2 \\ &= (x_p - x_t)^2 + (y_p - y_t)^2 + ((w_p - w_t)^2 + (h_p - h_t)^2) / 4 \\ &= l_2\text{-norm}(\Delta x, \Delta y, \Delta w/2, \Delta h/2) \end{aligned}$$

Wasserstein Distance



Wasserstein Distance

- 通用公式：

$$\mathbf{D}_w(\mathcal{N}_p, \mathcal{N}_t)^2 = \underbrace{\|\boldsymbol{\mu}_p - \boldsymbol{\mu}_t\|_2^2}_{\text{center distance}} + \underbrace{\text{Tr}(\boldsymbol{\Sigma}_p + \boldsymbol{\Sigma}_t - 2(\boldsymbol{\Sigma}_p^{1/2} \boldsymbol{\Sigma}_t \boldsymbol{\Sigma}_p^{1/2})^{1/2})}_{\text{coupling terms about } h_p, w_p \text{ and } \theta_p}$$

- 水平特殊情况：

$$\begin{aligned} \mathbf{D}_w^h(\mathcal{N}_p, \mathcal{N}_t)^2 &= \|\boldsymbol{\mu}_p - \boldsymbol{\mu}_t\|_2^2 + \|\boldsymbol{\Sigma}_p^{1/2} - \boldsymbol{\Sigma}_t^{1/2}\|_F^2 \\ &= (x_p - x_t)^2 + (y_p - y_t)^2 + ((w_p - w_t)^2 + (h_p - h_t)^2) / 4 \\ &= l_2\text{-norm}(\Delta x, \Delta y, \Delta w/2, \Delta h/2) \end{aligned}$$

- 损失函数

$$L_{gwd} = 1 - \frac{1}{\tau + f(\mathbf{D}_w^2)}, \quad \tau \geq 1$$

Kullback-Leibler Divergence

- 通用公式：

$$\mathbf{D}_{kl}(\mathcal{N}_p || \mathcal{N}_t) = \underbrace{\frac{1}{2}(\boldsymbol{\mu}_p - \boldsymbol{\mu}_t)^\top \boldsymbol{\Sigma}_t^{-1}(\boldsymbol{\mu}_p - \boldsymbol{\mu}_t)}_{\text{term about } x_p \text{ and } y_p} + \underbrace{\frac{1}{2}\text{Tr}(\boldsymbol{\Sigma}_t^{-1}\boldsymbol{\Sigma}_p) + \frac{1}{2}\ln \frac{|\boldsymbol{\Sigma}_t|}{|\boldsymbol{\Sigma}_p|}}_{\text{coupling terms about } h_p, w_p \text{ and } \theta_p} - 1$$

或

$$\mathbf{D}_{kl}(\mathcal{N}_t || \mathcal{N}_p) = \underbrace{\frac{1}{2}(\boldsymbol{\mu}_p - \boldsymbol{\mu}_t)^\top \boldsymbol{\Sigma}_p^{-1}(\boldsymbol{\mu}_p - \boldsymbol{\mu}_t) + \frac{1}{2}\text{Tr}(\boldsymbol{\Sigma}_p^{-1}\boldsymbol{\Sigma}_t) + \frac{1}{2}\ln \frac{|\boldsymbol{\Sigma}_p|}{|\boldsymbol{\Sigma}_t|}}_{\text{chain coupling of all parameters}} - 1$$

- 水平特殊情况：

$$\begin{aligned} \mathbf{D}_{kl}^h(\mathcal{N}_p || \mathcal{N}_t) &= \frac{1}{2} \left(\frac{w_p^2}{w_t^2} + \frac{h_p^2}{h_t^2} + \frac{4\Delta^2 x}{w_t^2} + \frac{4\Delta^2 y}{h_t^2} + \ln \frac{w_t^2}{w_p^2} + \ln \frac{h_t^2}{h_p^2} - 2 \right) \\ &= 2l_2\text{-norm}(\Delta t_x, \Delta t_y) + l_1\text{-norm}(\Delta t_w, \Delta t_h) + \frac{1}{2}l_2\text{-norm}\left(\frac{1}{\Delta t_w}, \frac{1}{\Delta t_h}\right) - 1 \end{aligned}$$

高精度分析 (KLD>GWD>smooth L1) :

- KLD主要三项的具体表达式 :

$$(\boldsymbol{\mu}_p - \boldsymbol{\mu}_t)^\top \boldsymbol{\Sigma}_t^{-1} (\boldsymbol{\mu}_p - \boldsymbol{\mu}_t) = \frac{4(\Delta x \cos \theta_t + \Delta y \sin \theta_t)^2}{w_t^2} + \frac{4(\Delta y \cos \theta_t - \Delta x \sin \theta_t)^2}{h_t^2}$$

$$\mathbf{Tr}(\boldsymbol{\Sigma}_t^{-1} \boldsymbol{\Sigma}_p) = \frac{h_p^2}{w_t^2} \sin^2 \Delta \theta + \frac{w_p^2}{h_t^2} \sin^2 \Delta \theta + \frac{h_p^2}{h_t^2} \cos^2 \Delta \theta + \frac{w_p^2}{w_t^2} \cos^2 \Delta \theta$$

$$\ln \frac{|\boldsymbol{\Sigma}_t|}{|\boldsymbol{\Sigma}_p|} = \ln \frac{h_t^2}{h_p^2} + \ln \frac{w_t^2}{w_p^2}$$

其中 $\Delta x = x_p - x_t$, $\Delta y = y_p - y_t$, $\Delta \theta = \theta_p - \theta_t$ 。

高精度分析 (KLD>GWD>smooth L1) :

- 不失一般性, 我们令 $\theta_t=0$, 对KLD的 μ_p 求导数:

$$\frac{\partial \mathbf{D}_{kl}(\mu_p)}{\partial \mu_p} = \left(\frac{4}{w_t^2} \Delta x, \frac{4}{h_t^2} \Delta y \right)^\top$$

- 当 $\theta_t \neq 0$ 时, 目标的偏移量 (Δx 和 Δy) 的梯度会根据角度进行动态调整以提供更好的优化。相比之下, GWD和 L2关于偏移量的梯度分别是:

$$\frac{\partial \mathbf{D}_w(\mu_p)}{\partial \mu_p} = (2\Delta x, 2\Delta y)^\top$$

$$\frac{\partial L_2(\mu_p)}{\partial \mu_p} = \left(\frac{2}{w_a^2} \Delta x, \frac{2}{h_a^2} \Delta y \right)^\top$$

高精度分析 (KLD>GWD>smooth L1) :

- 对KLD的 h_p 和 w_p 求导数 :

$$\frac{\partial \mathbf{D}_{kl}(\boldsymbol{\Sigma}_p)}{\partial \ln h_p} = \frac{h_p^2}{h_t^2} \cos^2 \Delta\theta + \frac{h_p^2}{w_t^2} \sin^2 \Delta\theta - 1, \quad \frac{\partial \mathbf{D}_{kl}(\boldsymbol{\Sigma}_p)}{\partial \ln w_p} = \frac{w_p^2}{w_t^2} \cos^2 \Delta\theta + \frac{w_p^2}{h_t^2} \sin^2 \Delta\theta - 1$$

- 我们可以看到, 两边 h_p 和 w_p 梯度和角度差 $\Delta\theta$ 有关。当 $\Delta\theta=0$ 时 :

$$\frac{\partial \mathbf{D}_{kl}(\boldsymbol{\Sigma}_p)}{\partial \ln h_p} = \frac{h_p^2}{h_t^2} - 1, \quad \frac{\partial \mathbf{D}_{kl}(\boldsymbol{\Sigma}_p)}{\partial \ln w_p} = \frac{w_p^2}{w_t^2} - 1$$

- 这意味着较小的目标尺度会导致其匹配到更大的损失。这是符合认知的, 因为较小的边需要更高的匹配精度。

高精度分析 (KLD>GWD>smooth L1) :

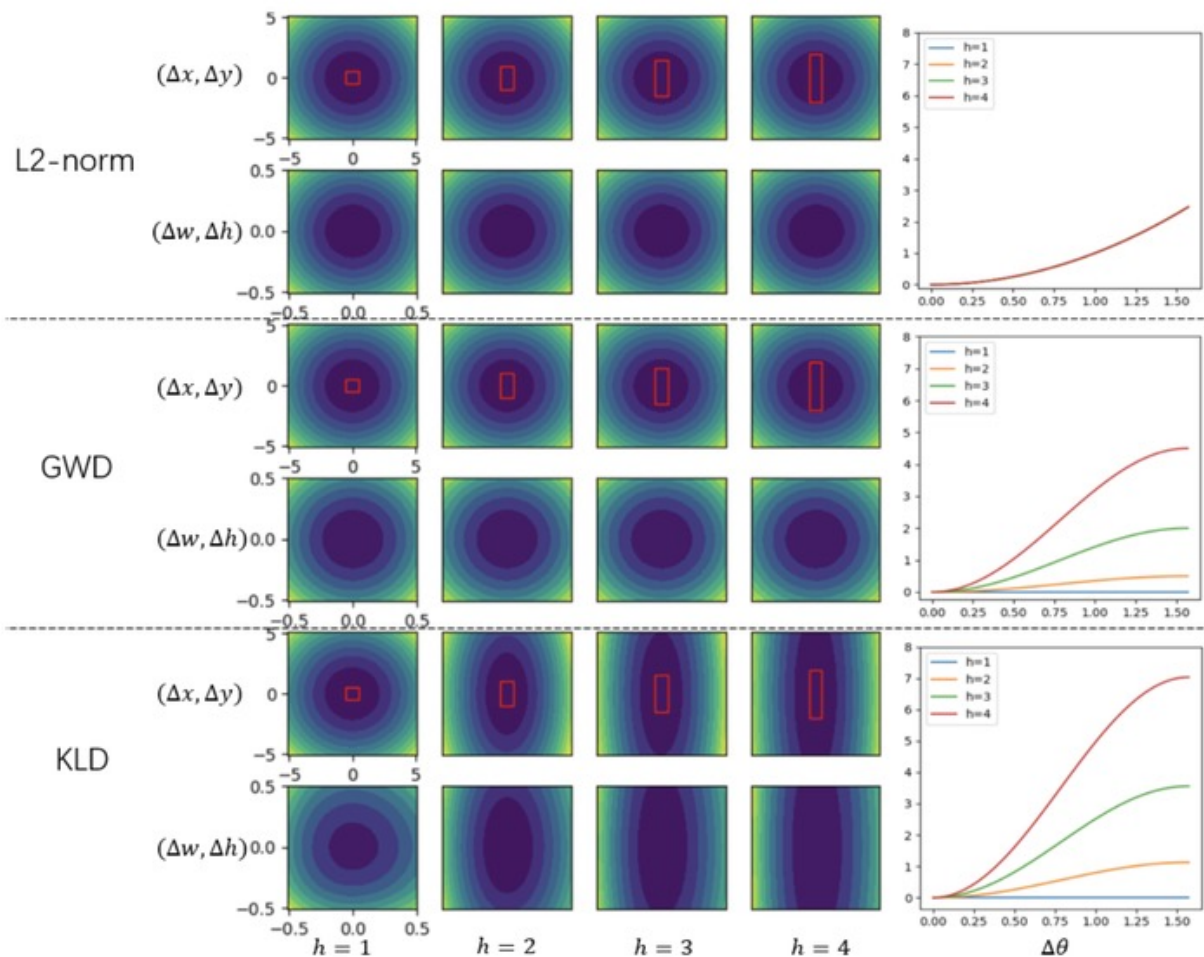
- 对 θ 求导数：
$$\frac{\partial \mathbf{D}_{kl}(\boldsymbol{\Sigma}_p)}{\partial \theta_p} = \left(\frac{h_p^2 - w_p^2}{w_t^2} + \frac{w_p^2 - h_p^2}{h_t^2} \right) \sin 2\Delta\theta$$

- 角度差 $\Delta\theta$ 的优化又和两边 h_p 和 w_p 有关。当 $h_p=h_t$, $w_p=w_t$ 时：

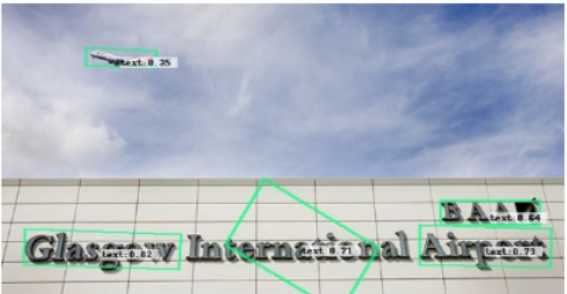
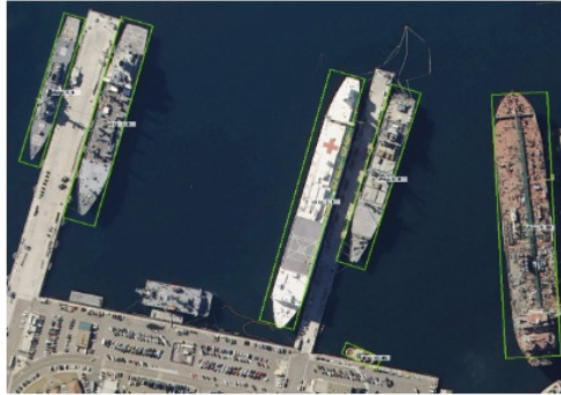
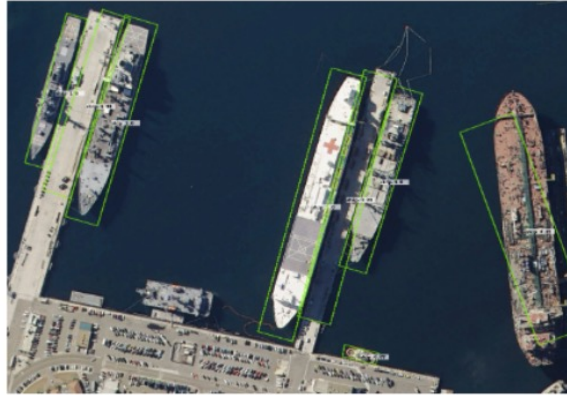
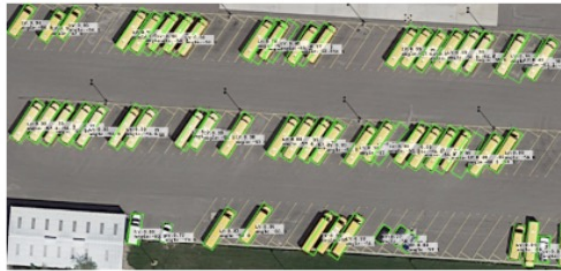
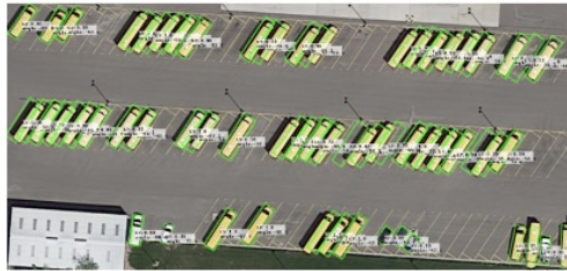
$$\frac{\partial \mathbf{D}_{kl}(\boldsymbol{\Sigma}_p)}{\partial \theta_p} = \left(\frac{h_t^2}{w_t^2} + \frac{w_t^2}{h_t^2} - 2 \right) \sin 2\Delta\theta \geq \sin 2\Delta\theta$$

- 当目标长宽比慢慢变大的时候，整个式子的值就会变大，也就是意味着对角度优化更加看重。这个优化机制是非常好的，我们知道对于长宽比越大的目标来说，它受角度差的影响就越大，IoU会产生急剧下降。

高精度分析 (KLD>GWD>smooth L1) :



高精度分析 (KLD>GWD>smooth L1) :



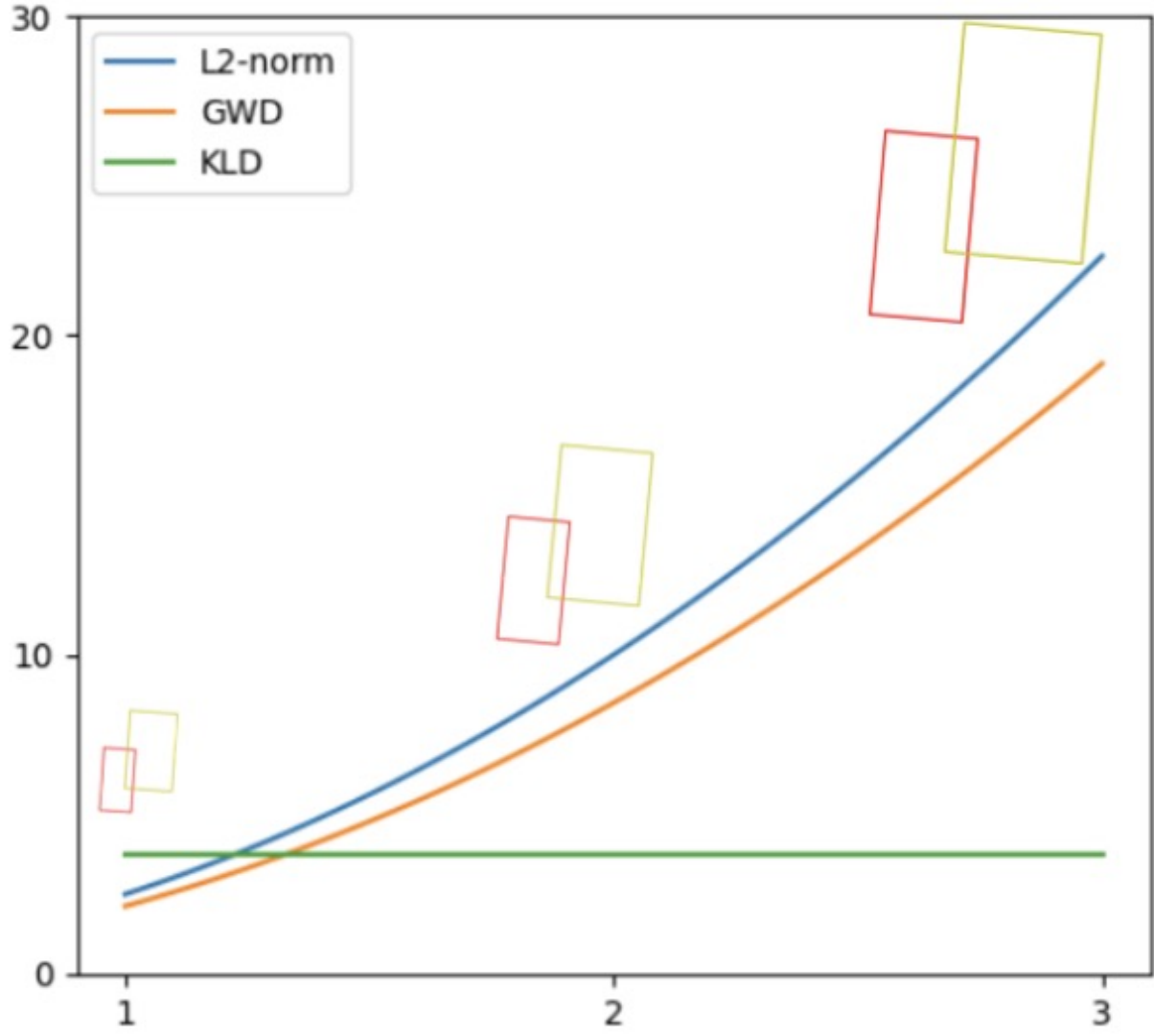
尺度不变性证明

- 很明显GWD和 L_2 不具有尺度不变性。
- 对于两个已知的高斯分布 $\mathbf{X}_p \sim \mathcal{N}_p(\boldsymbol{\mu}_p, \boldsymbol{\Sigma}_p)$ 和 $\mathbf{X}_t \sim \mathcal{N}_t(\boldsymbol{\mu}_t, \boldsymbol{\Sigma}_t)$, 假设有一个满秩的矩阵 \mathbf{M} ($|\mathbf{M}| \neq 0$), 有: $\mathbf{X}_{p'} = \mathbf{M}\mathbf{X}_p \sim \mathcal{N}_p(\mathbf{M}\boldsymbol{\mu}_p, \mathbf{M}\boldsymbol{\Sigma}_p\mathbf{M}^\top)$, $\mathbf{X}_{t'} = \mathbf{M}\mathbf{X}_t \sim \mathcal{N}_t(\mathbf{M}\boldsymbol{\mu}_t, \mathbf{M}\boldsymbol{\Sigma}_t\mathbf{M}^\top)$
- 我们将其分别标记为 $\mathcal{N}_{p'}$ 和 $\mathcal{N}_{t'}$, 那么它们的KLD计算如下:

$$\begin{aligned} \mathbf{D}_{kl}(\mathcal{N}_{p'} || \mathcal{N}_{t'}) &= \frac{1}{2}(\boldsymbol{\mu}_p - \boldsymbol{\mu}_t)^\top \mathbf{M}^\top (\mathbf{M}^\top)^{-1} \boldsymbol{\Sigma}_t^{-1} \mathbf{M}^{-1} \mathbf{M}(\boldsymbol{\mu}_p - \boldsymbol{\mu}_t) \\ &\quad + \frac{1}{2} \text{Tr} ((\mathbf{M}^\top)^{-1} \boldsymbol{\Sigma}_t^{-1} \mathbf{M}^{-1} \mathbf{M} \boldsymbol{\Sigma}_p \mathbf{M}^\top) + \frac{1}{2} \ln \frac{|\mathbf{M}| |\boldsymbol{\Sigma}_t| |\mathbf{M}^\top|}{|\mathbf{M}| |\boldsymbol{\Sigma}_p| |\mathbf{M}^\top|} - 1 \\ &= \frac{1}{2}(\boldsymbol{\mu}_p - \boldsymbol{\mu}_t)^\top \boldsymbol{\Sigma}_t^{-1} (\boldsymbol{\mu}_p - \boldsymbol{\mu}_t) + \frac{1}{2} \text{Tr} (\mathbf{M}^\top (\mathbf{M}^\top)^{-1} \boldsymbol{\Sigma}_t^{-1} \mathbf{M}^{-1} \mathbf{M} \boldsymbol{\Sigma}_p) + \frac{1}{2} \ln \frac{|\boldsymbol{\Sigma}_t|}{|\boldsymbol{\Sigma}_p|} - 1 \\ &= \mathbf{D}_{kl}(\mathcal{N}_p || \mathcal{N}_t) \end{aligned}$$

- 因此KLD具有仿射不变性的。当 $\mathbf{M} = k\mathbf{I}$ 时, KLD的尺度不变性就被证明了。

尺度不变性比较



在3种数据集和2种检测器上进行了高精度检测实验，KLD具有绝对优势。

Table 4: High-precision detection experiment under different regression loss. ‘R’, ‘F’ and ‘G’ indicate random rotation, flipping, and graying, respectively. The resolution of HRSC2016, MSRA-TD500 and ICDAR2015 are 500×500 , $800 \times 1,000$ and $800 \times 1,000$, respectively.

Method	Dataset	Data Aug.	Reg. Loss	Hmean ₅₀ /AP ₅₀	Hmean ₆₀ /AP ₆₀	Hmean ₇₅ /AP ₇₅	Hmean ₈₅ /AP ₈₅	Hmean _{50:95} /AP _{50:95}
RetinaNet	HRSC2016	R+F+G	Smooth L1	84.28	74.74	48.42	12.56	47.76
			GWD	85.56 (+1.28)	84.04 (+9.30)	60.31 (+11.89)	17.14 (+4.58)	52.89 (+5.13)
			KLD	87.45 (+3.17)	86.72 (+11.98)	72.39 (+23.97)	27.68 (+15.12)	57.80 (+10.04)
R ³ Det		R+F+G	Smooth L1	88.52	79.01	43.42	4.58	46.18
			GWD	89.43 (+0.91)	88.89 (+9.88)	65.88 (+22.46)	15.02 (+10.44)	56.07 (+9.89)
			KLD	89.97 (+1.45)	89.73 (+10.72)	77.38 (+33.96)	25.12 (+20.54)	61.40 (+15.22)
RetinaNet	MSRA-TD500	R+F	Smooth L1	70.98	62.42	36.73	12.56	37.89
			GWD	76.76 (+5.78)	68.58 (+6.16)	44.21 (+7.48)	17.75 (+5.19)	43.62 (+5.73)
			KLD	76.96 (+5.98)	70.08 (+7.66)	46.95 (+10.22)	19.59 (+7.03)	45.24 (+7.35)
	R+F	F	Smooth L1	69.78	64.15	36.97	8.71	37.73
			GWD	74.29 (+4.51)	68.34 (+4.19)	43.39 (+6.42)	10.50 (+1.79)	41.68 (+3.95)
			KLD	75.32 (+5.54)	69.94 (+5.79)	44.46 (+7.49)	10.70 (+1.99)	42.68 (+4.95)
R ³ Det	ICDAR2015	R+F	Smooth L1	74.83	69.46	42.02	11.59	41.98
			GWD	76.15 (+1.32)	71.26 (+1.80)	45.59 (+3.57)	11.65 (+0.06)	43.58 (+1.60)
			KLD	77.92 (+3.09)	72.77 (+3.31)	43.27 (+1.25)	11.09 (-0.50)	43.65 (+1.67)
	F	R+F	Smooth L1	74.28	68.12	35.73	8.01	39.10
			GWD	75.59 (+1.31)	68.36 (+0.24)	40.24 (+4.51)	9.15 (+1.14)	40.80 (+1.70)
			KLD	77.72 (+2.43)	71.99 (+3.87)	43.95 (+8.22)	10.43 (+2.42)	43.29 (+4.19)
R+F	R+F	Smooth L1	75.53	69.69	37.69	9.03	40.56	
		GWD	77.09 (+1.56)	71.52 (+1.83)	41.08 (+3.39)	10.10 (+1.07)	42.17 (+1.61)	
		KLD	79.63 (+4.63)	73.30 (+3.61)	43.51 (+5.82)	10.61 (+1.58)	43.61 (+3.05)	

我们在一些更具有挑战性的数据集上进行了验证实验，包括DOTA-v1.5和DOTA-v2.0（包含很多像素值小于10的目标），KLD依旧表现出色。

Table 6: Accuracy comparison between different rotation detectors on DOTA dataset. \dagger and \ddagger represent the large aspect ratio object and the square-like object, respectively. The bold red and blue fonts indicate the top two performances respectively. D_{oc} and D_{le} represent OpenCV Definition ($\theta \in [-90^\circ, 0^\circ)$) and Long Edge Definition ($\theta \in [-90^\circ, 90^\circ)$) of RBox.

Baseline	Method	Box Def.	v1.0 tranval/test								v1.0 train/val			v1.5	v2.0	
			BR \dagger	SV \dagger	LV \dagger	SH \dagger	HA \dagger	ST \ddagger	RA \ddagger	7-AP $_{50}$	AP $_{50}$	AP $_{50}$	AP $_{75}$	AP $_{50:95}$	AP $_{50}$	AP $_{50}$
RetinaNet	-	D_{oc}	42.17	65.93	51.11	72.61	53.24	78.38	62.00	60.78	65.73	64.70	32.31	34.50	58.87	44.16
	-	D_{le}	38.31	60.48	49.77	68.29	51.28	78.60	60.02	58.11	64.17	62.21	26.06	31.49	56.10	43.06
	IoU-Smooth L1 [3]	D_{oc}	44.32	63.03	51.25	72.78	56.21	77.98	63.22	61.26	66.99	64.61	34.17	36.23	59.16	46.31
	Modulated Loss [46]	D_{oc}	42.92	67.92	52.91	72.67	53.64	80.22	58.21	61.21	66.05	63.50	33.32	34.61	57.75	45.17
	Modulated Loss [46]	Quad.	43.21	70.78	54.70	72.68	60.99	79.72	62.08	63.45	67.20	65.15	40.59	39.12	61.42	46.71
	RIL [35]	Quad.	40.81	67.63	55.45	72.42	55.49	78.09	64.75	62.09	66.06	64.07	40.98	39.05	58.91	45.35
	CSL [4]	D_{le}	42.25	68.28	54.51	72.85	53.10	75.59	58.99	60.80	67.38	64.40	32.58	35.04	58.55	43.34
	DCL (BCL) [47]	D_{le}	41.40	65.82	56.27	73.80	54.30	79.02	60.25	61.55	67.39	65.93	35.66	36.71	59.38	45.46
	GWD [5]	D_{oc}	44.07	71.92	62.56	77.94	60.25	79.64	63.52	65.70	68.93	65.44	38.68	38.71	60.03	46.65
KLD	D_{oc}	44.00	74.45	72.48	84.30	65.54	80.03	65.05	69.41	71.28	68.14	44.48	42.15	62.50	47.69	
R ³ Det	-	D_{oc}	44.15	75.09	72.88	86.04	56.49	82.53	61.01	68.31	70.66	67.18	38.41	38.46	62.91	48.43
	DCL (BCL) [47]	D_{le}	46.84	74.87	74.96	85.70	57.72	84.06	63.77	69.70	71.21	67.45	35.44	37.54	61.98	48.71
	GWD [5]	D_{oc}	46.73	75.84	78.00	86.71	62.69	83.09	61.12	70.60	71.56	69.28	43.35	41.56	63.22	49.25
	KLD	D_{oc}	48.34	75.09	78.88	86.52	65.48	82.08	61.51	71.13	71.73	68.87	44.48	42.11	65.18	50.90

在水平检测任务上（COCO数据集），KLD也是和GIoU等常见损失函数保持差不多的水平。

Table 6: Performance evaluation of KLD on classic horizontal detection.

Detector	Reg. Loss	AP	AP ₅₀	AP ₇₅	AP _s	AP _m	AP _l	Detector	Reg. Loss	AP	AP ₅₀	AP ₇₅	AP _s	AP _m	AP _l
RetinaNet	Smooth L1	37.2	56.6	39.7	21.4	41.1	48.0	Faster RCNN	Smooth L1	37.9	58.8	41.0	22.4	41.4	49.1
	GIoU	37.4	56.7	39.7	22.2	41.7	48.1		GIoU	38.3	58.7	41.5	22.5	41.7	49.7
	KLD	38.0	56.4	40.6	23.3	43.2	49.3		KLD	38.2	58.7	41.7	22.6	41.8	49.3

我们对KLD不同变体在两个数据集上进行了实验，发现最后的效果是差不多的，排除了不对称性对结果的干扰。

Table 2: Ablation of different KLD-based regression loss form. The based detector is RetinaNet.

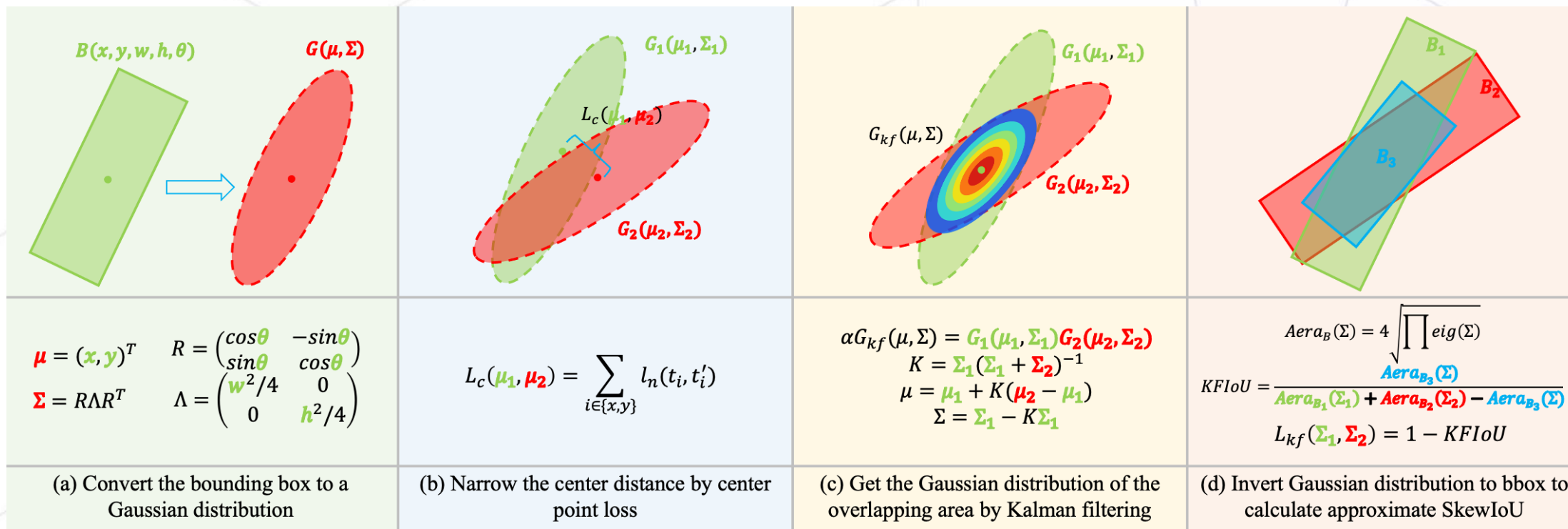
Dataset	$D_{kl}(\mathcal{N}_p \mathcal{N}_t)$	$D_{kl}(\mathcal{N}_t \mathcal{N}_p)$	$D_{kl_min}(\mathcal{N}_p \mathcal{N}_t)$	$D_{kl_max}(\mathcal{N}_p \mathcal{N}_t)$	$D_{js}(\mathcal{N}_p \mathcal{N}_t)$	$D_{jeffreys}(\mathcal{N}_p \mathcal{N}_t)$
DOTA-v1.0	70.17	70.64	70.71	70.55	69.67	70.56
HRSC2016	82.83	83.82	83.60	82.70	84.06	83.66

最后在DOTA-v1.0的SOTA实验中，我们也取得了当前所发表论文里的最高性能。

Table 8: AP on different objects on DOTA-v1.0. Here R-101 denotes ResNet-101 (likewise for R-50, R-152), and RX-101 and H-104 represent ResNeXt101 [50] and Hourglass-104 [51], respectively. MS indicates that multi-scale training/testing is used. **Red** and **blue** indicate the top two performances.

	Method	Backbone	MS	PL	BD	BR	GTF	SV	LV	SH	TC	BC	ST	SBF	RA	HA	SP	HC	AP ₅₀
Two-stage	ICN [32]	R-101	✓	81.40	74.30	47.70	70.30	64.90	67.80	70.00	90.80	79.10	78.20	53.60	62.90	67.00	64.20	50.20	68.20
	RoI-Trans. [12]	R-101	✓	88.64	78.52	43.44	75.92	68.81	73.68	83.59	90.74	77.27	81.46	58.39	53.54	62.83	58.93	47.67	69.56
	SCRDet [3]	R-101	✓	89.98	80.65	52.09	68.36	68.36	60.32	72.41	90.85	87.94	86.86	65.02	66.68	66.25	68.24	65.21	72.61
	Gliding Vertex [52]	R-101		89.64	85.00	52.26	77.34	73.01	73.14	86.82	90.74	79.02	86.81	59.55	70.91	72.94	70.86	57.32	75.02
	Mask OBB [53]	RX-101	✓	89.56	85.95	54.21	72.90	76.52	74.16	85.63	89.85	83.81	86.48	54.89	69.64	73.94	69.06	63.32	75.33
	CenterMap OBB [54]	R-101	✓	89.83	84.41	54.60	70.25	77.66	78.32	87.19	90.66	84.89	85.27	56.46	69.23	74.13	71.56	66.06	76.03
	FPN-CSL [4]	R-152	✓	90.25	85.53	54.64	75.31	70.44	73.51	77.62	90.84	86.15	86.69	69.60	68.04	73.83	71.10	68.93	76.17
	RSDet-II [46]	R-152	✓	89.93	84.45	53.77	74.35	71.52	78.31	78.12	91.14	87.35	86.93	65.64	65.17	75.35	79.74	63.31	76.34
	SCRDet++ [55]	R-101	✓	90.05	84.39	55.44	73.99	77.54	71.11	86.05	90.67	87.32	87.08	69.62	68.90	73.74	71.29	65.08	76.81
	ReDet [56]	ReR-50	✓	88.81	82.48	60.83	80.82	78.34	86.06	88.31	90.87	88.77	87.03	68.65	66.90	79.26	79.71	74.67	80.10
Single-stage	PloU [33]	DLA-34 [57]		80.90	69.70	24.10	60.20	38.30	64.40	64.80	90.90	77.20	70.40	46.50	37.10	57.10	61.90	64.00	60.50
	H-104		✓	89.31	82.14	47.33	61.21	71.32	74.03	78.62	90.76	82.23	81.36	60.93	60.17	58.21	66.98	61.03	71.04
	O ² -DNet [58]	R-101	✓	88.61	79.69	46.27	70.37	65.89	76.10	78.53	90.84	79.98	78.41	58.71	62.02	69.23	71.32	60.65	71.78
	DAL [15]	R-101	✓	88.58	77.83	50.44	69.29	71.10	75.79	78.66	90.88	80.10	81.71	57.92	63.03	66.30	69.77	63.13	72.30
	P-RSDet [59]	R-101	✓	88.35	79.96	50.69	62.18	78.43	78.98	87.94	90.85	83.58	84.35	54.13	60.24	65.22	64.28	55.70	72.32
	BBAVectors [60]	R-101	✓	89.71	82.34	47.22	64.10	76.22	74.43	85.84	90.57	86.18	84.89	57.65	61.93	69.30	69.63	58.48	73.23
	DRN [14]	H-104	✓	89.71	82.34	47.22	64.10	76.22	74.43	85.84	90.57	86.18	84.89	57.65	61.93	69.30	69.63	58.48	73.23
	PolarDet [61]	R-101	✓	89.65	87.07	48.14	70.97	78.53	80.34	87.45	90.76	85.63	86.87	61.64	70.32	71.92	73.09	67.15	76.64
	RDD [62]	R-101	✓	89.15	83.92	52.51	73.06	77.81	79.00	87.08	90.62	86.72	87.15	63.96	70.29	76.98	75.79	72.15	77.75
	GWD [5]	R-152	✓	89.06	84.32	55.33	77.53	76.95	70.28	83.95	89.75	84.51	86.06	73.47	67.77	72.60	75.76	74.17	77.43
Refine-stage	KLD	R-50		88.91	83.71	50.10	68.75	78.20	76.05	84.58	89.41	86.15	85.28	63.15	60.90	75.06	71.51	67.45	75.28
		R-50	✓	88.91	85.23	53.64	81.23	78.20	76.99	84.58	89.50	86.84	86.38	71.69	68.06	75.95	72.23	75.42	78.32
	CFC-Net [34]	R-101	✓	89.08	80.41	52.41	70.02	76.28	78.11	87.21	90.89	84.47	85.64	60.51	61.52	67.82	68.02	50.09	73.50
	R ³ Det [29]	R-152	✓	89.80	83.77	48.11	66.77	78.76	83.27	87.84	90.82	85.38	85.51	65.67	62.68	67.53	78.56	72.62	76.47
	DAL [15]	R-50	✓	89.69	83.11	55.03	71.00	78.30	81.90	88.46	90.89	84.97	87.46	64.41	65.65	76.86	72.09	64.35	76.95
	DCL [47]	R-152	✓	89.26	83.60	53.54	72.76	79.04	82.56	87.31	90.67	86.59	86.98	67.49	66.88	73.29	70.56	69.99	77.37
	RIDet [35]	R-50	✓	89.31	80.77	54.07	76.38	79.81	81.99	89.13	90.72	83.58	87.22	64.42	67.56	78.08	79.17	62.07	77.62
	S ² A-Net [13]	R-101	✓	89.28	84.11	56.95	79.21	80.18	82.93	89.21	90.86	84.66	87.61	71.66	68.23	78.58	78.20	65.55	79.15
	R ³ Det-GWD [5]	R-152	✓	89.66	84.99	59.26	82.19	78.97	84.83	87.70	90.21	86.54	86.85	73.04	67.56	76.92	79.22	74.92	80.19
		R-50		88.90	84.17	55.80	69.35	78.72	84.08	87.00	89.75	84.32	85.73	64.74	61.80	76.62	78.49	70.89	77.36
	R-50	✓	89.90	84.91	59.21	78.74	78.82	83.95	87.41	89.89	86.63	86.69	70.47	70.87	76.96	79.40	78.62	80.17	
	R-152	✓	89.92	85.13	59.19	81.33	78.82	84.38	87.50	89.80	87.33	87.00	72.57	71.35	77.12	79.34	78.68	80.63	

基于高斯的SkewIoU近似，KFIoU



趋势一致性分析

$$E\text{Mean} = \frac{1}{N} \sum_{i=1}^N (\text{SkewIoU}_{plain} - \text{SkewIoU}_{app}),$$

$$E\text{Var} = \frac{1}{N} \sum_{i=1}^N (\text{SkewIoU}_{app} - E\text{Mean})^2$$

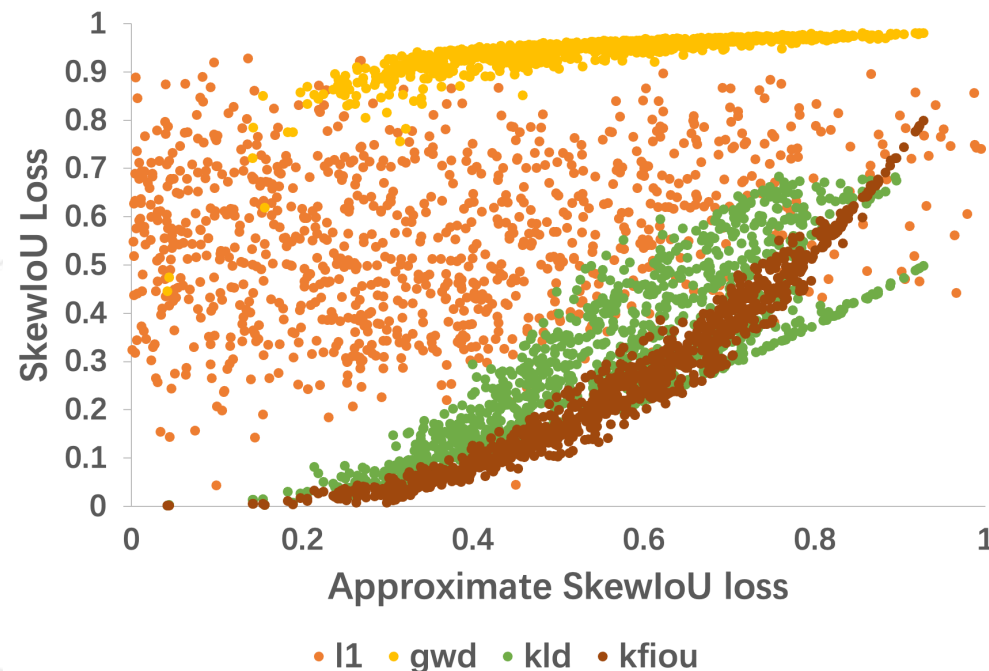
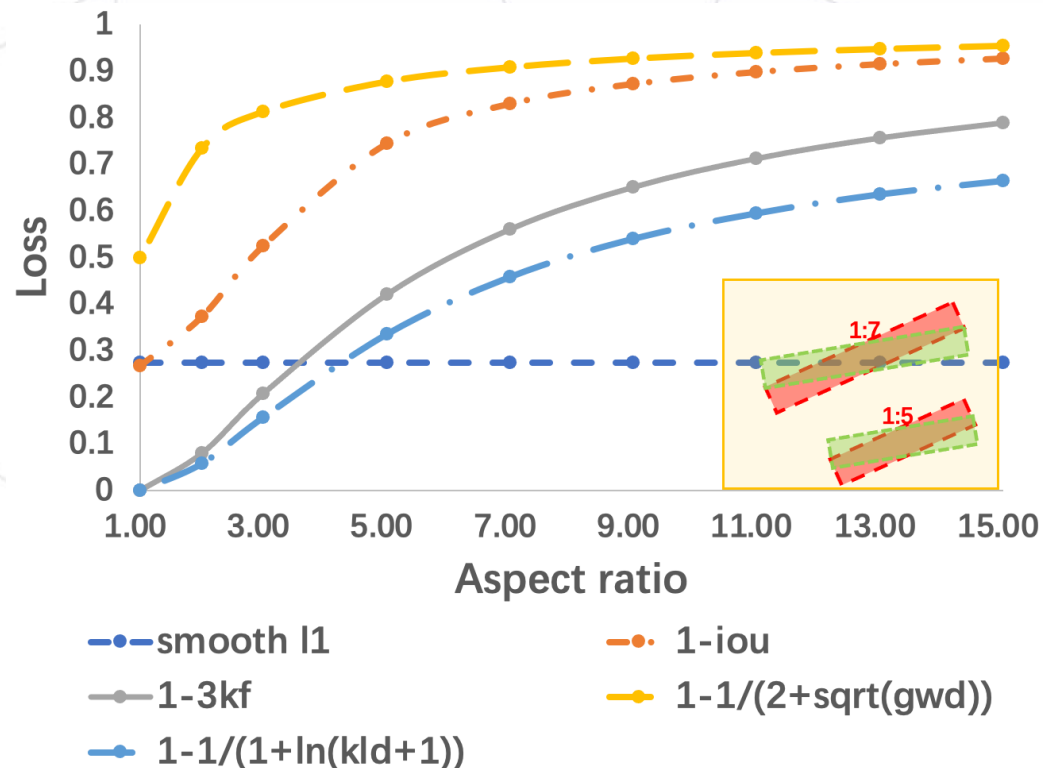
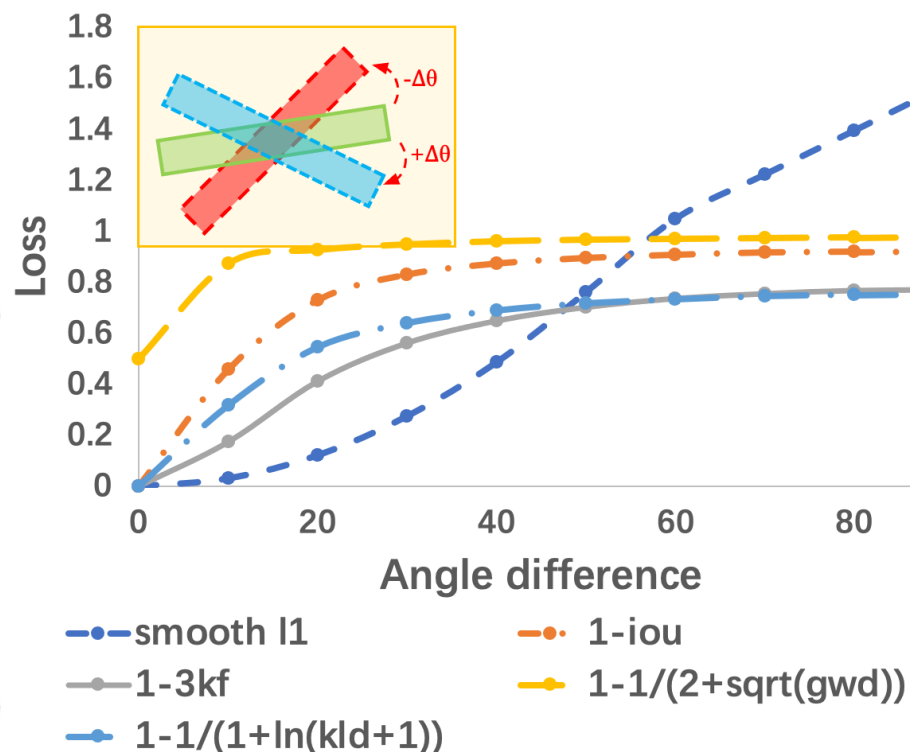


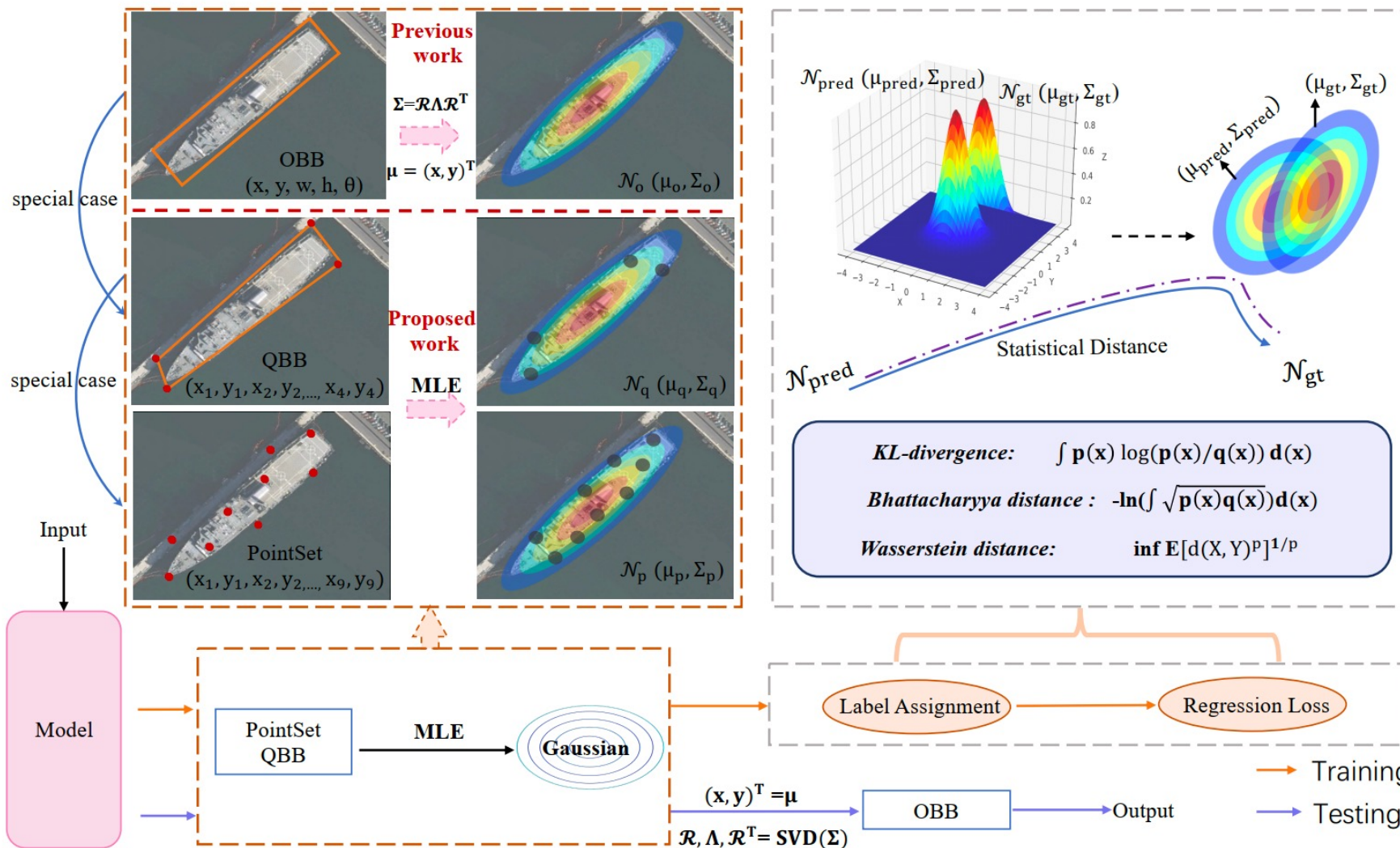
Table 1: Comparison of the properties and performance of different regression losses. Base model is RetinaNet. **BC**, **SI** and **HP** denote Boundary Continuity, Scale Invariance and Hyperparameter.

Loss	Representation	Implement	BC	SI	Consistency	HP	EVar [↓]	DOTA-v1.0	DOTA-v1.5	DOTA-v2.0
Smooth L1	bbox	easy	×	×	×	✓ (σ)	0.073201718	64.17	56.10	43.06
plain SkewIoU	bbox	hard	✓	✓	✓	×	-	68.27	59.01	45.87
GWD	Gaussian	easy	✓	×	×	✓ (τ)	0.019041297	68.93	60.03	46.65
KLD	Gaussian	easy	✓	✓	✓	✓ (τ)	0.007653582	71.28	62.50	47.69
KFIoU (ours)	Gaussian	easy	✓	✓	✓	×	0.002348353	70.64	62.71	48.04

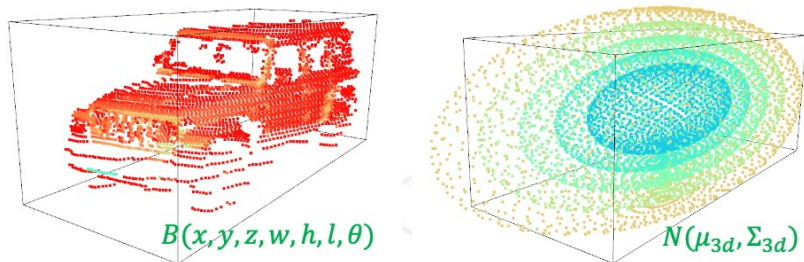
趋势一致性分析



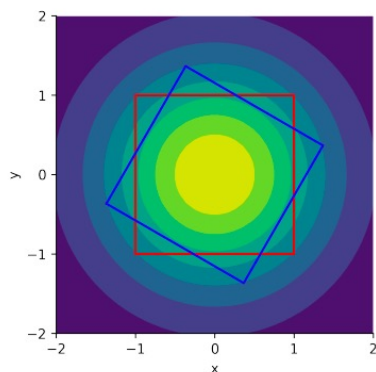
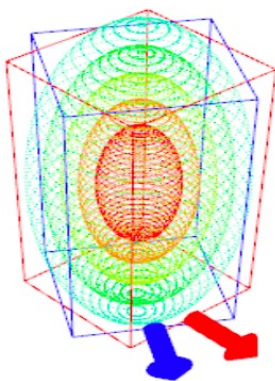
高斯建模后续扩展工作——G-Rep



高斯建模后续扩展工作——3D目标检测

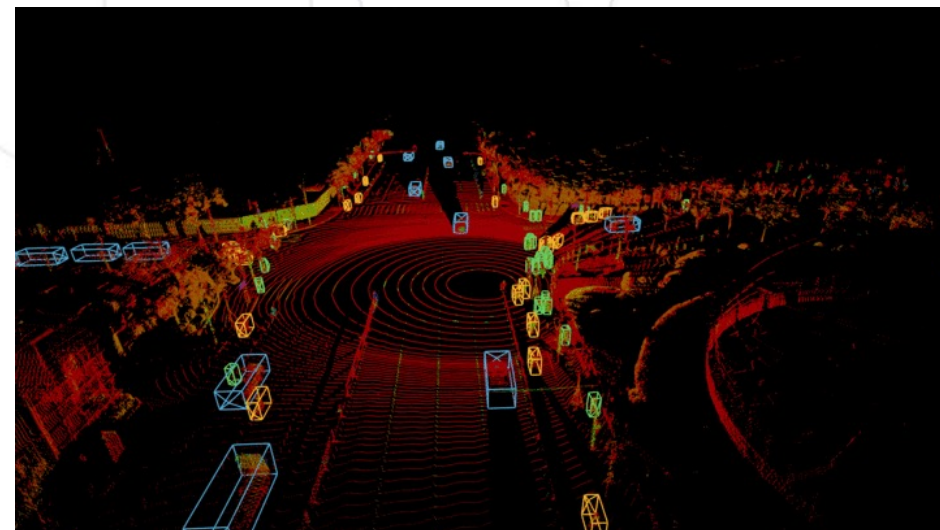
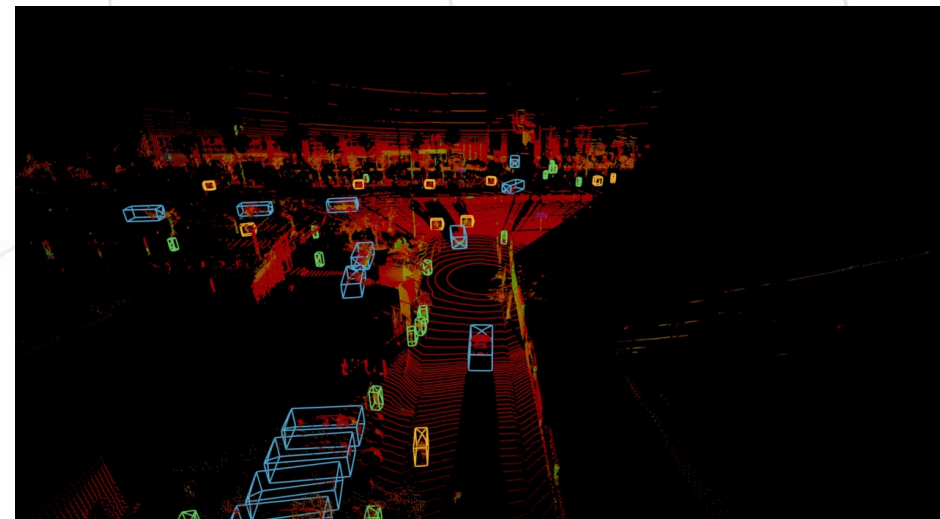


3D高斯表示



(b) 3-D BBox with square shape in top-view e.g. pedestrian. (c) Top view of the 3-D BBox and the heading is arbitrary given the isotropic 2-D Gaussian.

类正方形退化问题



MMRotate : 基于PyTorch的有向检测工具



OpenMMLab website *HOT* OpenMMLab platform *TRY IT OUT*

docs passing build passing codecov unknown pypi v0.3.0 license Apache-2.0 issue resolution 3 h open issues 100%

[Documentation](#) | [Installation](#) | [Model Zoo](#) | [Reporting Issues](#)

AlphaRotate : 基于TensorFlow的有向检测工具

AlphaRotate: A Rotation Detection Benchmark using TensorFlow

docs passing pypi package 1.0.1 downloads 1k License Apache 2.0 issue resolution 2 d open issues 14%

<https://github.com/open-mmlab/mmrrotate>

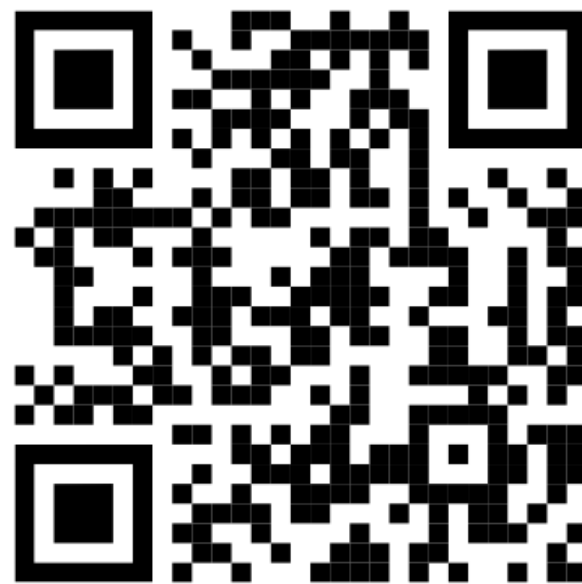
<https://github.com/yangxue0827/RotationDetection>

谢谢！

Q & A



扫码添加小助手
备注“社区开放麦”
加入讨论群
和大佬lvl



扫码查看主页
了解更多我的
研究内容